

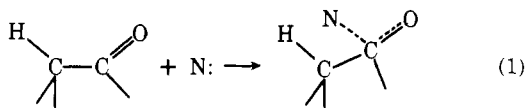
The β -Hydrogen Secondary Isotope Effect in Acyl Transfer Reactions. Origins, Temperature Dependence, and Utility as a Probe of Transition-State Structure¹

Ildiko M. Kovach, John L. Hogg, Tony Raben, Kevin Halbert,
James Rodgers, and Richard L. Schowen*

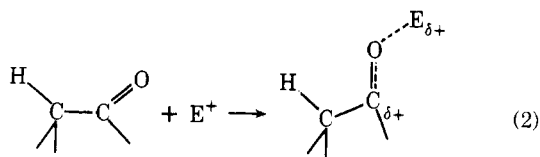
Contribution from the Department of Chemistry, University of Kansas,
Lawrence, Kansas 66045. Received August 8, 1979

Abstract: The anomalous temperature dependence of the β -deuterium (β -D) secondary isotope effect reported by Halevi and Margolin for the hydroxide-promoted hydrolysis of ethyl acetate has been observed also with methyl acetate [$\text{CH}_3\text{CO}_2\text{CH}_3$ vs. $\text{CD}_3\text{CO}_2\text{CH}_3$: $k_{3\text{H}}/k_{3\text{D}} = 1.01 \pm 0.02$ (0 °C), 0.90 ± 0.02 (25 °C), 1.03 ± 0.10 (50 °C)]. In contrast, the β -D effects for the rates of acidic hydrolysis of methyl acetate (0.93 ± 0.02 , 0–42 °C), basic hydrolysis of phenyl acetate (0.98 ± 0.02 , 5–45 °C), basic methanolysis of *p*-methoxyphenyl acetate (0.96 ± 0.02 , 5–45 °C), and the equilibrium hydration of 1,3-dichloroacetone ($\text{ClCH}_2\text{COCH}_2\text{Cl}$ vs. $\text{ClCD}_2\text{COCDCl}$: $K_{4\text{H}}/K_{4\text{D}} = 0.83 \pm 0.02$, 15–46 °C) over the indicated temperature ranges were statistically indistinguishable from the mean values cited. This constitutes “regular”, expected behavior. Both kinds of cases are consistent with a cascade model for acyl-transfer reactions in which solvent-reorganization and heavy-atom-reorganization transition states along parallel reaction paths alternate in dominating rate limitation in the 0–70 °C temperature range. Such a model also explains anomalous temperature dependences of solvent isotope effects for anhydride hydrolyses, reported by Rossall and Robertson. Observed transition-state properties would refer to a virtual, weighted-average, transition-state structure, according to the cascade model.

The utility of the β -hydrogen secondary isotope effect for investigating acyl-transfer transition-state structures in both enzymic and nonenzymic reactions^{2,3} could in principle be as great as it has been for nucleophilic-substitution reactions at saturated carbon.^{4,5} Although small steric⁶ and polar (“inductive”) contributions may be present,⁷ this effect can reasonably be expected to arise almost entirely from changes in β -CH force constants induced by variations in hyperconjugation of the electrons of the β -CH bonds into the carbonyl group.⁸ An increase in nucleophilic interaction at carbonyl carbon (eq 1) should decrease such hyperconjugation, in-



creasing the force constants and producing an inverse isotope effect ($k_{\text{H}} < k_{\text{D}}$). An increased electrophilic interaction at carbonyl oxygen (eq 2) should increase the positive charge at



carbonyl carbon and increase hyperconjugation of the β -CH bonding electrons. This should decrease the force constants and produce a normal isotope effect ($k_{\text{H}} > k_{\text{D}}$).⁹ The direction and magnitude of such an effect should therefore be diagnostic of transition-state nucleophilic and electrophilic interactions at the carbonyl group.^{10,11}

This is exactly the view taken by Bender and his collaborators in their initial exploration of this mechanistic probe in acyl-transfer reactions around 20 years ago.^{12,13} However, a complication of the simple picture was discovered by Halevi and Margolin¹⁴ when they investigated the temperature dependence of the β -hydrogen isotope effect for the basic hydrolysis of ethyl acetate ($\text{CH}_3\text{CO}_2\text{CH}_2\text{CH}_3$ vs. $\text{CD}_3\text{CO}_2\text{CH}_2\text{CH}_3$). Bender and Feng¹² found $k_{3\text{H}}/k_{3\text{D}} = 0.90 \pm 0.01$ for this reaction at 25 °C, suggesting a predominance of nucleophilic interaction in the transition state, as expected for a quasi-tetrahedral structure. But, as Halevi and Margolin

showed, this effect is observed only in the range 20–35 °C. At lower temperatures the effect drifts toward 1.0, while at 65 °C a normal effect $k_{3\text{H}}/k_{3\text{D}} = 1.15 \pm 0.09$ is obtained.

Such a temperature dependence is anomalous. If the hyperconjugative picture outlined above were correct, if a single transition state were important over the temperature range from 0 to 65 °C, and if the dominant origin of the isotope effect were changes in zero-point energy, then an effect of 0.90 at 25 °C might have been expected to change only to 0.89 at 0 °C and to 0.91 at 65 °C. The extreme changes and, indeed, crossing over of inverse to normal effects are therefore contrary to expectation. The anomalous temperature dependence may have two simple kinds of explanation.

Theoretical investigations of anomalous temperature dependences,^{15–19} including the “crossover” of inverse to normal isotope effects as the temperature is varied, have shown that certain combinations of force-constant changes on conversion of reactants to transition state may produce isotope-effect minima, maxima, and other divergences from a simple monotonic decrease in magnitude with increasing temperature. In a vibrational-analysis calculation closely related to the situation under discussion here, Wolfsberg and Stern¹⁵ constructed a set of force fields which generated a slightly U-shaped temperature dependence of the β -hydrogen isotope effect in a model for $\text{S}_{\text{N}}1$ solvolysis of an isopropyl halide. Their force fields (set up merely for illustrative purposes and not asserted to be physically probable) involved a drop of the β -CH stretching force constant by about 30% (4.8 to 3.5 mdyn/Å) concomitant with large rises in low force constants, by 570% (0.15 to 1.00 mdyn/Å) for an HCCC torsion and by 50% (0.68 to 1.00 mdyn/Å) for an HCC bend, when the reactant molecule went to the transition state. The result was an isotope effect $k_{6\text{H}}/k_{6\text{D}}$ at 100 K of 1.47, chiefly from zero-point energy sources (MMI = 1.00, EXC = 1.09, ZPE = 1.35),²⁰ an effect at 250 K of 1.41, arising both from zero-point energy sources and from vibrational excitation (MMI = 1.00, EXC = 1.25, ZPE = 1.13), and an effect at 380 K of 1.42 which came mostly from excitation (MMI = 1.00, EXC = 1.31, ZPE = 1.08). They noted that “a fairly wide range of force constants can give rise to such temperature dependences”.

If this kind of force-constant change is responsible for the ethyl acetate β -hydrogen effect, then it will not necessarily be valid to infer from the isotope effect, by means of simple

comparisons and direct analogies to related systems, the structural features of the transition state. On the other hand, as Vogel and Stern¹⁹ suggested, "Because of the strong force-field sensitivity of anomalous regions of calculated temperature-dependence curves, fitting such a region to experimental data should provide a fairly unambiguous result in terms of the force-constant changes occurring between reactant(s) and transition state." That is to say, what is lost in the value of empirical analogy may be made up in the structural precision which would be demanded of a model calculation that successfully described the data.

However, these peculiar force fields are not the only possible origin of an anomalous temperature dependence for a kinetic isotope effect. Thornton²² mentioned the finding of Halevi and Margolin¹⁴ in a review of 1966 as "possibly implying a change in mechanism", or, as of course one could add, a change in rate-determining step or both. For small perturbations of the free energy of activation, such as secondary isotope effects, it is readily shown²³ that eq 3 describes the effect on the observed free energy of activation ΔG_o^\ddagger in the terms of each of the free-energy changes for conversion of reactants to the i th of the activated complexes, ΔG_i^\ddagger .

$$\delta\Delta G_o^\ddagger = \sum_i w_i \delta\Delta G_i^\ddagger \quad (3)$$

The weighting factors w_i depend in form upon whether the contributing activated complexes occur along a common route in series (competing rate-determining steps) or along independent parallel routes (competing mechanisms). Along a serial pathway, the form of w_i is given by eq 4a, and along parallel paths by eq 4b.

$$\text{serial: } w_i = \exp(\Delta G_i^\ddagger/RT)/\exp(\Delta G_o^\ddagger/RT) \quad (4a)$$

$$\text{parallel: } w_i = \exp(-\Delta G_i^\ddagger/RT)/\exp(-\Delta G_o^\ddagger/RT) \quad (4b)$$

For small isotope effects for which $\delta\Delta G_i^\ddagger$ is much smaller than ΔG_i^\ddagger for either the light or heavy isotopic species, so that eq 3 is valid with regular (i.e., nonanomalous) temperature dependences, the *apparent* temperature dependence of the isotope effect will come from the temperature dependences of the w_i (which may be taken as derived from the light-isotopic species). If the isotope effects for the individual steps or mechanistic paths, $\delta\Delta G_i^\ddagger$, differ considerably, and if the ΔH_i^\ddagger also differ considerably, then dramatic swings of the apparent isotope effect may occur over limited ranges of temperature. In the present paper, we will present kinetic models of this kind, capable of matching the observations for a number of anomalous isotope effects in acyl-transfer reactions.

From a strictly empirical point of view, it is clear that a large number of nucleophilic reactions at carbonyl centers conform to the expectation of an inverse β -hydrogen isotope effect. Inverse effects of 0.99–0.91 per deuterium at or near 25 °C have been observed for more than 20 examples of rates and equilibria by a number of investigators.^{12,13,24–28} Nevertheless, the Halevi–Margolin observation is not unique. Congdon and Edward²⁵ have found somewhat similar dependences for basic hydrolysis of 1-acetyl-5,5-dimethyl-2-thiohydantoin ($k_{3H}/k_{3D} = 1.00$ at 11 and 58 °C, 0.97 at 25 °C with labeled acetyl group) and for hydrolysis of the same substrate in 39.6% sulfuric acid (0.95 at 11 °C, 0.93 at 25.3 °C, 1.13 at 49.6 °C). Rossall and Robertson²⁹ observed maxima in the *solvent* isotope effects for neutral hydrolysis of acetic anhydride (2.83 at 0 °C, 2.94 at 15 °C, 2.98 at 30 °C), succinic anhydride (2.57 at 0 °C, 2.75 at 30 °C, 2.74 at 40 °C), and phthalic anhydride (2.26 at 0 °C, 2.32 at 15 °C, 2.20 at 25 °C), while minima in the solvent isotope effect appeared with propionic anhydride (3.19 at 0 °C, 2.74 at 30 °C, 2.95 at 50 °C) and benzoic anhydride (3.66 at 10 °C, 2.92 at 50 °C, 2.97 at 60 °C).³⁰ Acetic anhydride hydrolysis is particularly notable in this series, since

Bender and Feng¹² found $k_{6H}/k_{6D} = 1.00$ at 25 °C for this reaction. More recently, Küllertz, Fischer, and Barth²⁷ measured CH_3/CD_3 effects in the basic hydrolysis of *p*-nitroacetanilide, finding a "reasonable" value of 0.87 ± 0.05 for k_{3H}/k_{3D} at high concentrations of base where attack of hydroxide to generate the tetrahedral adduct is probably³¹ rate limiting, but an "anomalous" value of 1.08 ± 0.04 at low hydroxide concentrations, where decomposition of the tetrahedral intermediate, probably with general acid catalysis by the solvent,^{31,32} limits the rate.

We have examined the temperature dependence of the β -hydrogen isotope effect for some nucleophilic reactions of acetyl esters and for a ketone equilibrium hydration reaction. We want to consider the results in the light of the findings already discussed, with a view toward deciding the likely utility of this effect as a probe of transition-state structure.

Results

Basic Hydrolysis of Methyl Acetate. In Table I are given second-order rate constants for the hydrolysis in basic solution (initial sodium hydroxide concentration 0.01 M) of $CH_3CO_2CH_3$ and $CD_3CO_2CH_3$ at temperatures from 0 to 50 °C, and the corresponding isotope effects. The values of k_{3H} at 0 and 25 °C can be compared with those measured by Fairclough and Hinshelwood³³ (29.8×10^{-3} and $152 \times 10^{-3} \text{ M}^{-1} \text{ s}^{-1}$, respectively); the agreement is good. The isotope effect at 25 °C is exactly equal to that found for the basic hydrolysis of ethyl acetate by Bender and Feng¹² while the effects at 0 and 35 °C are in agreement with those for ethyl acetate (1.00 ± 0.01 and 0.93 ± 0.01) as determined by Halevi and Margolin.¹⁴ The unusual temperature dependence observed for the basic hydrolysis of ethyl acetate is thus repeated exactly in the basic hydrolysis of methyl acetate.

Acidic Hydrolysis of Methyl Acetate. Table II contains first-order rate constants for the hydrolysis in 0.1160 M aqueous perchloric acid of $CH_3CO_2CH_3$ and $CD_3CO_2CH_3$ at temperatures from 0 to 42 °C, together with the corresponding isotope effects. The ratio of the first-order rate constant to stoichiometric concentration of perchloric acid at 15.1 °C is $3.75 \times 10^{-5} \text{ M}^{-1} \text{ s}^{-1}$. This may be compared to similar ratios, at 15 °C, of $2.23 \times 10^{-5} \text{ M}^{-1} \text{ s}^{-1}$ for the reaction in 1.439 N sulfuric acid³⁴ and $4.90 \times 10^{-5} \text{ M}^{-1} \text{ s}^{-1}$ for the reaction in 1.317 M hydrochloric acid.³⁵ The isotope effects reported in Table II are all inverse and near their mean value of $k_{3H}/k_{3D} = 0.93 \pm 0.02$, calculated for the entire temperature range of 0–42 °C. If an isotope effect of 0.93 at 25 °C were to arise wholly from a difference in enthalpies of activation (a simple, "regular" model of temperature dependence), the value would change only to 0.924 at 0 °C and to 0.934 at 42 °C and thus the temperature dependence would be undetectable with errors of 2%. Here the higher and lowest mean isotope effects for individual temperatures lie within one standard deviation of the mean value for all temperatures, a result which is consistent with the simplest "regular" expectation and also with any other model which predicts variations only within about 2%.

Basic Hydrolysis of Phenyl Acetate. Second-order rate constants and isotope effects for the reaction of hydroxide ion with phenyl acetate ($CH_3CO_2C_6H_5$ and $CD_3CO_2C_6H_5$) appear in Table III. Within the level of precision attained, no variation in the isotope effect could be detected, with all values being indistinguishable (within one standard deviation) from the mean of 0.976 ± 0.025 .

Basic Methanolysis of Aryl Acetates. Tables IV and V show second-order rate constants and isotope effects for reactions of methoxide ion in methanol with phenyl acetate ($CH_3CO_2C_6H_5$ and $CD_3CO_2C_6H_5$) and the corresponding isotopic *p*-methoxyphenyl acetates, respectively. Here again no temperature variation beyond the limit of about 2% could

Table I. Second-Order Rate Constants and Isotope Effects for the Hydrolysis of $\text{CH}_3\text{CO}_2\text{CH}_3$ and $\text{CD}_3\text{CO}_2\text{CH}_3$ in Aqueous 0.01 M Sodium Hydroxide Solutions

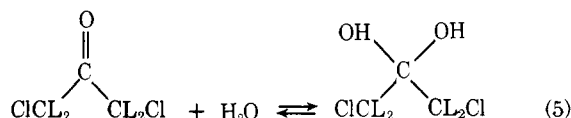
temp, °C	$10^3 k_{3\text{H}}$, $\text{M}^{-1} \text{s}^{-1}$, ± SD	$10^3 k_{3\text{D}}$, $\text{M}^{-1} \text{s}^{-1}$, ± SD	$k_{3\text{H}}/k_{3\text{D}}$ ± SD
0.0 ± 0.1	28.9 ± 0.5	28.7 ± 0.5	1.01 ± 0.02
15.0 ± 0.1	83.1 ± 0.9	85.3 ± 0.8	0.95 ± 0.01
25.00 ± 0.05	152 ± 3	169 ± 2	0.90 ± 0.02
35.0 ± 0.1	286 ± 6	311 ± 7	0.92 ± 0.03
50.0 ± 0.1	472 ± 34	460 ± 29	1.03 ± 0.10

Table II. First-Order Rate Constants and Isotope Effects for the Hydrolysis of $\text{CH}_3\text{CO}_2\text{CH}_3$ and $\text{CD}_3\text{CO}_2\text{CH}_3$ in Aqueous Solutions of 0.1160 M Perchloric Acid

temp, °C	$10^7 k_{3\text{H}}$, s^{-1} , ± SD	$10^7 k_{3\text{D}}$, s^{-1} , ± SD	$k_{3\text{H}}/k_{3\text{D}}$ ± SD
0.0 ± 0.1	8.83 ± 0.13	9.58 ± 0.14	0.92 ± 0.02
15.1 ± 0.1	43.5 ± 0.5	47.0 ± 0.6	0.93 ± 0.02
30.00 ± 0.05	200 ± 2	213 ± 2	0.94 ± 0.02
30.10 ± 0.05	204 ± 2	215 ± 2	0.95 ± 0.02
40.00 ± 0.05	462 ± 5	495 ± 5	0.93 ± 0.01
42.00 ± 0.05	578 ± 12	621 ± 12	0.93 ± 0.02

be detected, the mean isotope effects for the entire temperature ranges being 0.976 ± 0.018 (5–45 °C) for phenyl acetate and 0.962 ± 0.023 (5–45 °C) for *p*-methoxyphenyl acetate.

Hydration of 1,3-Dichloroacetone. The equilibrium constants for hydration of the protiated and deuterated forms of 1,3-dichloroacetone (eq 5, L = H or D) at temperatures from



15 to 46 °C are shown in Table VI. The values were determined spectrophotometrically, assuming for each isotopic ketone that the extinction coefficient at the absorption maximum in water (273 nm) was the same as that at the absorption maximum in acetonitrile (282 nm), and that the hydrate did not absorb at these wavelengths. Greenzaid, Rappoport, and Samuel³⁶ used a linear correlation of extinction coefficients for chloroacetone and 1,3-dichloroacetone at their absorption maxima in various solvents to estimate a value for 1,3-dichloroacetone in water. This value is equal to that for acetonitrile, so the procedure should be valid. Our values of $K_{4\text{H}}$ (from measurements at 273 nm) are consistently 3–17% smaller than those calculated by Greenzaid, Rappoport, and Samuel³⁶ from absorption data at 270 nm of Bell and McDougall.³⁷ This doubtless reflects small differences in the true extinction coefficients at the two wavelengths, to which the equilibrium constants are sensitive. The isotope effects are totally insensitive to the extinction coefficient; however, values of ϵ around 26 were used in the calculations, and, while in one case $K_{4\text{H}}$ is calculated to be 4.90 for ϵ 20 and 8.44 for ϵ 32, $K_{\text{H}}/K_{\text{D}}$ is calculated to be 0.84 for ϵ 20 and 0.85 for ϵ 32. Thus, while the individual values of $K_{4\text{H}}$ and $K_{4\text{D}}$ in Table III are quite dependent on the methodological assumptions, the isotope effects are not and should be very reliable. The effects exhibit no detectable dependence on temperature, being indistinguishable from their mean value of 0.83 ± 0.02 .

Discussion

It seems a fair summary of the experimental findings reported here to note that (a) only the basic hydrolysis of methyl acetate displays a β -D isotope-effect temperature dependence which is clearly anomalous; (b) the equilibrium hydration of 1,3-dichloroacetone and the rates of acidic hydrolysis of methyl

Table III. Second-Order Rate Constants^a and Isotope Effects for the Basic Hydrolysis of $\text{CL}_3\text{CO}_2\text{C}_6\text{H}_5$ in Water at Various Temperatures

temp, °C	$10^3 k_{3\text{H}}$, $\text{M}^{-1} \text{s}^{-1}$, ± SD	$10^3 k_{3\text{D}}$, $\text{M}^{-1} \text{s}^{-1}$, ± SD	$k_{3\text{H}}/k_{3\text{D}}$ ± SD
5.00 ± 0.01	314 ± 5	324 ± 7	0.970 ± 0.028
10.00 ± 0.01	455 ± 3	467 ± 3	0.974 ± 0.008
15.00 ± 0.01	674 ± 5	689 ± 7	0.980 ± 0.012
25.00 ± 0.01	1309 ± 9	1336 ± 9	0.980 ± 0.009
45.00 ± 0.01	4078 ± 108	4156 ± 118	0.981 ± 0.038

^a From least-squares fitting of 3–15 replicate pairwise determinations of first-order rate constants in aqueous solutions of sodium hydroxide at 4–5 different concentrations from 0.0080 to 0.0400 M.

Table IV. Second-Order Rate Constants^a and Isotope Effects for the Basic Methanolysis of $\text{CL}_3\text{CO}_2\text{C}_6\text{H}_5$ in Methanol at Various Temperatures

temp, °C	$10^3 k_{3\text{H}}$, $\text{M}^{-1} \text{s}^{-1}$, ± SD	$10^3 k_{3\text{D}}$, $\text{M}^{-1} \text{s}^{-1}$, ± SD	$k_{3\text{H}}/k_{3\text{D}}$ ± SD
5.00 ± 0.01	694 ± 10	700 ± 9	0.992 ± 0.019
10.00 ± 0.01	1038 ± 8	1050 ± 11	0.988 ± 0.013
15.00 ± 0.01	1445 ± 14	1494 ± 15	0.967 ± 0.014
20.00 ± 0.01	1687 ± 21	1750 ± 30	0.964 ± 0.020
25.00 ± 0.01	2829 ± 30	2928 ± 41	0.966 ± 0.017
30.00 ± 0.01	3983 ± 31	4122 ± 40	0.966 ± 0.012
35.00 ± 0.01	5903 ± 79	6112 ± 98	0.966 ± 0.020
37.60 ± 0.01	7169 ± 35	7273 ± 50	0.986 ± 0.008
40.00 ± 0.01	7460 ± 110	7531 ± 101	0.990 ± 0.021

^a From least-squares fitting of 3–15 replicate pairwise determinations (CH_3 and CD_3 substrates in alternation) of first-order rate constants in methanolic solutions of sodium methoxide at 4–5 different concentrations from 0.0040 to 0.0425 M.

Table V. Second-Order Rate Constants^a and Isotope Effects for the Basic Methanolysis of *p*- $\text{CH}_3\text{OC}_6\text{H}_4\text{O}_2\text{CCL}_3$ in Methanol at Various Temperatures

temp, °C	$10^3 k_{3\text{H}}$, $\text{M}^{-1} \text{s}^{-1}$, ± SD	$10^3 k_{3\text{D}}$, $\text{M}^{-1} \text{s}^{-1}$, ± SD	$k_{3\text{H}}/k_{3\text{D}}$ ± SD
5.00 ± 0.01	441 ± 6	456 ± 6	0.967 ± 0.019
10.00 ± 0.01	741 ± 7	764 ± 7	0.969 ± 0.012
15.00 ± 0.01	947 ± 16	984 ± 16	0.956 ± 0.023
25.00 ± 0.01	1936 ± 14	2031 ± 19	0.953 ± 0.011
35.00 ± 0.01	3527 ± 86	3678 ± 81	0.959 ± 0.032
45.00 ± 0.01	6560 ± 70	6770 ± 133	0.969 ± 0.022

^a From least-squares fitting of 3–15 replicate pairwise determinations (CH_3 and CD_3 substrates in alternation) of first-order rate constants in methanolic solutions of sodium methoxide at 4–5 different concentrations from 0.0054 to 0.0419 M.

acetate, basic hydrolysis of phenyl acetate, and basic methanolyses of phenyl and *p*-methoxyphenyl acetate all exhibit no detectable change in β -D effect, to within about $\pm 2\%$, within ± 10 –20 °C of room temperature (“regular,” nonanomalous results); (c) finally, although the errors prevent its specification, one is struck by an apparent tendency of the mean values of the observed β -D effects in some of the “regular” cases to drift in the direction of unity at high and low temperatures (see Tables IV–VI). When we take note of the earlier examples of anomalous effects cited in the Introduction, it would appear that, while obvious examples of anomalous β -D effects are not the rule in acyl-transfer and carbonyl-addition reactions, they do occur and they merit an explanation. It might furthermore be hoped that such an explanation would illuminate the mechanisms of all acyl-transfer reactions, including those with

Table VI. Equilibrium Constants and Isotope Effects for the Hydration of $\text{ClCH}_2\text{COCH}_2\text{Cl}$ and $\text{ClCD}_2\text{COCD}_2\text{Cl}$ in Aqueous Solution^a

temp, °C	$K_{4\text{H}}$	$K_{4\text{D}}$	$K_{4\text{H}}/K_{4\text{D}}$
15.0 ± 0.1	9.1 ± 0.2	10.7 ± 0.2	0.85 ± 0.02
25.00 ± 0.01 ^b	6.3 ± 0.1	7.9 ± 0.1	0.79 ± 0.02
	6.1 ± 0.1	7.5 ± 0.1	0.81 ± 0.01
	6.9 ± 0.1	8.1 ± 0.1	0.85 ± 0.02
	6.9 ± 0.2	8.3 ± 0.1	0.83 ± 0.03
		mean	0.82 ± 0.02
30.0 ± 0.1	5.2 ± 0.1	6.5 ± 0.1	0.80 ± 0.02
35.0 ± 0.1	4.30 ± 0.02	5.04 ± 0.04	0.85 ± 0.01
46.0 ± 0.1	2.89 ± 0.05	3.39 ± 0.03	0.86 ± 0.02

^a The standard state of water is taken as the pure liquid. ^b Pairwise determinations with protium and deuterium compounds are shown.

regularly behaved isotope effects, and would be of assistance in interpreting the magnitudes of their isotope effects.

A model based purely on force-constant effects along a single, one-step reaction pathway, in which a kind of circumstantial concatenation like that studied by Wolfsberg and Stern¹⁵ is postulated, will best be built upon careful vibrational analyses of the reactant acyl compounds and of model compounds, for activated complexes and intermediates, using spectra obtained in the relevant solvents. While the results of such a project are awaited, we want here to suggest a mechanistic model involving several transition states in series and parallel, which we consider capable of accounting for the results available to date.

Multiple Transition-State Model for Acyl Transfer. It seems very likely that most or all nucleophilic displacement reactions at acyl centers proceed through intermediate tetrahedral compounds so that at least two transition states (for formation and decomposition of the intermediate) occur along the reaction path. For most cases, this intermediate is of very low stability and it is frequently thought that the transition states occurring just before and just after it should both resemble the intermediate and thus each other closely.³⁸ Dramatic changes in reaction properties should therefore not result from changes in the rate-limiting role between these presumably very similar transition states. Indeed, their enthalpy of formation from reactants should—by this reasoning—be similar and, so far as temperature variation goes, no change from one to the other would be expected.

Other transition states besides these transition states for *internal heavy-atom reorganization* (HAR) must also lie along the reaction path, although their role in limiting the rate has sometimes been considered unimportant. For example, the nucleophile and acyl substrate must encounter each other (transport step). One or more stages may be required to remove solvent molecules from the space between the nucleophilic atom and the carbonyl carbon, and conceivably to arrange the solvent more favorably around the reacting functions (solvent reorganization (SR) steps, in part analogous to interconversion of the intimate, solvent-separated, and other ion pairs of solvolysis chemistry). Before, during, and after formation of the heavy-atom linkages of the tetrahedral adduct, the transfer of protons may occur (proton-transfer steps) and torsional and other motions may be required (internal relaxation steps). Further SR steps may be required to produce the equilibrium, properly solvated adduct (which may or may not actually lie on the main reaction route in the steady state). Then an entire corresponding panoply of processes must again be set in action to achieve decomposition of the adduct to product.

For the purposes of our model, we will consider the intervention of two serial transition states along a particular route of acyl transfer. They must differ substantially in β -D isotope effect, enthalpy of activation, and entropy of activation. For

concreteness, we shall formulate the model in terms of a solvent-reorganization (SR) step, followed by a bond-formation (HAR) step. However, other equivalent models—including ones for decomposition of the adduct or a combination of rate-determining formation and decomposition—can readily be imagined and could be made to fit the observations equally well.

We suppose that the two-step process of solvent reorganization followed by heavy-atom reorganization occurs along a number of similar, parallel routes. To make the argument concrete, we present the following specific version of the model. Along each of the routes, the SR step is considered to be very similar to the SR step along any other route, but to differ from its counterparts in the exact value of ΔS^\ddagger . The HAR steps are also taken as essentially the same along all routes except for the value of ΔS^\ddagger .

We imagine the SR processes to have the following characteristics: (1) a reasonably negative value of ΔS^\ddagger (say -50 to -65 eu), postulated to arise because solvent is being removed from nucleophilic sites on the nucleophile and electrophilic sites on the electrophilic carbonyl, leaving concentrated regions of high polarity; the resulting nonspecific dipolar attractions for solvent molecules should result in a constriction of the nearby solvent and net increase in tightness of solvation; (2) a reasonably low value of ΔH^\ddagger (say 2 kcal mol⁻¹), corresponding to the lack of internal bonding changes in either reactant, and to the postulated net condensation of solvent and thus a favorable solvation energy around the highly polar species preceding bond formation; (3) a normal value of the β -D isotope effect (say 1.1 – $1.2 = k_{3\text{H}}/k_{3\text{D}}$), from the increased hyperconjugation into the carbonyl as solvating water molecules are removed from the partially positive carbon.

The heavy-atom reorganization steps are considered to have these characteristics: (1) a rather positive value of ΔS^\ddagger (referred to the original reactants as initial reference state), of about -10 to $+5$ eu (The discharge of polarity as bonds form would cause release of the solvent molecules collected about the polar species preceding the bond-formation transition state. The combination of bimolecular reaction (negative entropy change) with release of solvent originally interacting strongly with the free electrophilic and nucleophilic reactants (positive entropy change) is postulated to result in a value of ΔS^\ddagger near zero.); (2) a large value of ΔH^\ddagger , around 20 kcal mol⁻¹, deriving from energetically costly changes in bonding and hybridization, etc., together with the desolvation energy required to release solvent molecules originally interacting with the electrophilic and nucleophilic reactants; (3) an inverse β -D isotope effect (perhaps 0.9 – $0.8 = k_{3\text{H}}/k_{3\text{D}}$) from loss of hyperconjugation as the nucleophilic bond formation proceeds.

Each of the parallel carbonyl-addition routes thus consists of a low- ΔH^\ddagger , negative- ΔS^\ddagger , SR step with normal β -D isotope effect and a high- ΔH^\ddagger , positive- ΔS^\ddagger , HAR step with inverse β -D isotope effect. One parallel route differs from another in the values of ΔS^\ddagger for the two steps: an SR step with an extremely negative ΔS^\ddagger (compared to other parallel SR steps) will be followed on its own reaction route specifically by an HAR step with an unusually positive ΔS^\ddagger , in comparison with its counterparts.⁴⁰ Correspondingly, other SR steps with less negative ΔS^\ddagger are followed by HAR steps with less positive ΔS^\ddagger .

The steady-state kinetic version of this model is given by the equation

$$k_o = \sum_i^m k_i; \quad k_i^{-1} = k_{Ai}^{-1} + k_{Bi}^{-1} \quad (6)$$

Here k_o is the observed rate constant, which is the summation of the rate constants k_i for reaction along m parallel routes. k_{Ai} is the rate constant for the SR step and k_{Bi} is the overall

rate constant (i.e., it is referred to the original reactants as initial reference state) for the HAR step.

The properties of the model can be simulated numerically as follows. Consider an acyl transfer reaction with four parallel routes (eq 6, $m = 4$), with all $\Delta H_{Ai}^\ddagger = 2 \text{ kcal mol}^{-1}$ and all $\Delta H_{Bi}^\ddagger = 20 \text{ kcal mol}^{-1}$. The entropies of activation are taken as

$$\Delta S_{Ai}^\ddagger = -45 - 5i \text{ eu}$$

$$\Delta S_{Bi}^\ddagger = -15 + 5i \text{ eu}$$

The β -D secondary isotope effects at 298 K (k_{3H}/k_{3D}) are taken as 1.3 for all the SR steps and 0.7 for all the HAR steps, with a purely enthalpic temperature dependence. Thus k_o (β -D), the observed rate constant for the triply deuterated substrate, is calculated from eq 6 with all parameters equal to those above, except that

$$\Delta H_{Ai}^\ddagger (\beta\text{-D}) = 2 + 298R \ln 1.3 \text{ kcal mol}^{-1}$$

$$\Delta H_{Bi}^\ddagger (\beta\text{-D}) = 20 + 298R \ln 0.7 \text{ kcal mol}^{-1}$$

To simulate the solvent isotope effects seen for anhydride hydrolysis by Rossall and Robertson,²⁹ we take $k_{H_2O}/k_{D_2O} = 1.5$ for the SR steps and 3.5 for the HAR steps, both at 298 K, with a purely enthalpic temperature dependence. Then k_o (D_2O) is obtained from eq 6 with the same values of ΔS^\ddagger as above but with

$$\Delta H_{Ai}^\ddagger (D_2O) = 2 + 298R \ln 1.5 \text{ kcal mol}^{-1}$$

$$\Delta H_{Bi}^\ddagger (D_2O) = 20 + 298R \ln 3.5 \text{ kcal mol}^{-1}$$

Figure 1 portrays this numerical simulation of the temperature dependences of the rate constants and isotope effects over the range from 250 to 500 K. Part (a) of the figure shows the Eyring plot. Although it is roughly linear ($\Delta H_{app}^\ddagger \sim 11 \text{ kcal mol}^{-1}$, $\Delta S_{app}^\ddagger \sim -31 \text{ eu}$), its undulatory character is easily visible and is more obvious when the data are plotted over a smaller temperature range. Nevertheless, it is clear that a complex mechanistic model with four parallel pathways, each with two steps, and with each of these eight steps achieving considerable importance in limiting the rate at some temperature, can still generate an almost linear Eyring plot. The individual breaks in the plot, although perhaps difficult to discern from the figure, can be identified with particular changes in rate-determining step and reaction pathway. At the high-temperature (left) side of Figure 1a, at 500 K, step A (SR) of pathway $i = 1$ is rate determining. At 450 K, the plot breaks downward as the rate-determining step changes to step B (HAR) of pathway $i = 1$; at 400 K, the plot breaks upward as step A (SR) of pathway $i = 2$ becomes rate limiting. Across the plot, changes in rate-determining step from step A to step B of the various pathways (downward breaks) occur at 450 ($i = 1$), 360 ($i = 2$), 300 ($i = 3$), and 257 K ($i = 4$). Changes from one parallel pathway to another (upward breaks) occur at 400 ($i = 1-2$), 327 ($i = 2-3$), and 277 K ($i = 3-4$). Of course, if other combinations of activation parameters had been chosen, the undulatory character of the quasi-linear plot could have been enhanced or suppressed.

In Figure 1b is shown the corresponding simulation for the β -D secondary isotope effect. As the rate-determining step oscillates between SR processes with $k_{3H}/k_{3D} = 1.3$ and HAR processes with $k_H/k_D = 0.7$, the observed isotope effect oscillates between normal values (but less than 1.3) and inverse values (but not less than 0.7). Even though the isotope effects were taken as wholly enthalpic in origin, the temperature dependence of such small effects is so nearly negligible that the oscillation seems to occur about a nearly constant mean value. It is plain that this kind of mechanistic model can generate maxima, minima, inflection points, or oscillations in kinetic isotope effect temperature dependences. If the isotope effects

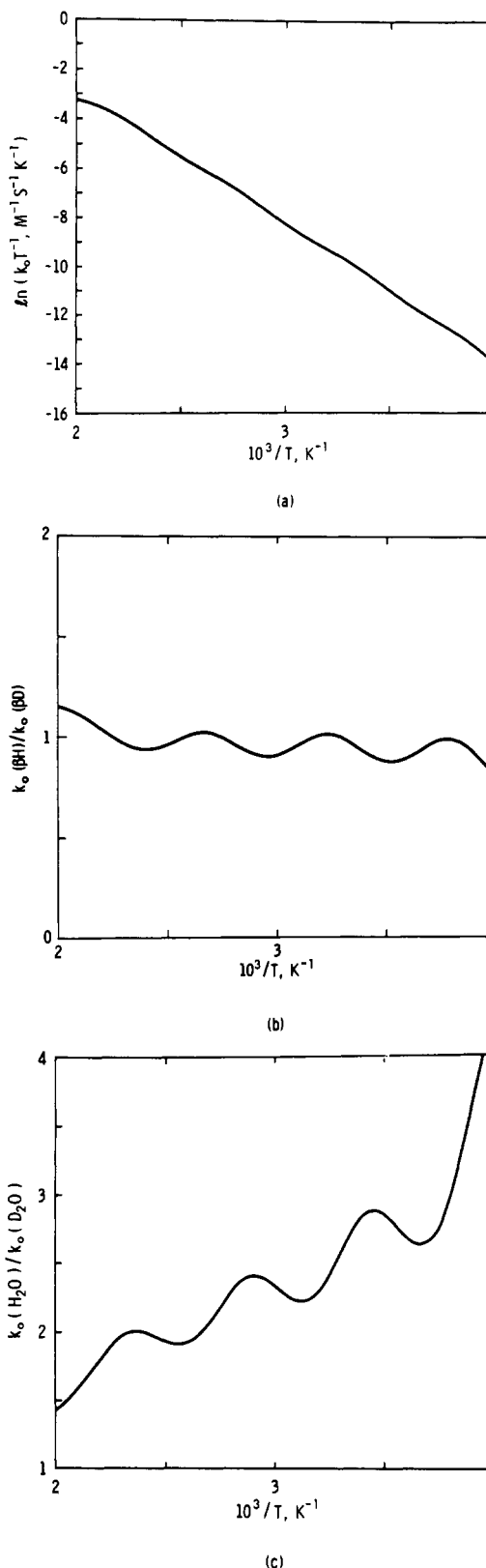


Figure 1. Calculated kinetic properties according to the model of eq 6 with parameters given in the text. (a) Eyring plot for β -H substrate in H_2O . (b) Temperature dependence of the β -D isotope effect. (c) Temperature dependence of the solvent isotope effect.

are quite different for the two types of rate-determining step, and if the activation parameters for the two types of step also differ greatly, the isotope-effect excursions can be striking over a temperature range where the nonlinearity of the Eyring plot is almost undetectable.

The simulation of the solvent isotope effects appears in Figure 1c. Here again the oscillatory character is apparent and, because the isotope effects assumed (1.5 at 298 K for SR steps, 3.5 at 298 K for HAR steps) are much larger, the effects rise as the temperature falls, giving a strong "tilt" to the plot. The geometric character of these oscillations is strikingly similar to that of the experimental curves for anhydride hydrolysis in Figure 1 of Rossall and Robertson's paper.²⁹ Indeed, our model can be considered simply an explicit version of the concept of "temperature-dependent solvation effects and . . . the related effect on partitioning" of intermediates which these authors suggested²⁹ in the explanation of their findings.

We conclude from this numerical simulation, in which ΔS^\ddagger is used to control a cascade among a number of transition states in series and parallel, that vigorous swings in the magnitude and direction of kinetic isotope effects can be produced by temperature-induced changes in pathway and rate-determining step, under conditions such that the nonlinear character of the Eyring plot is not necessarily readily apparent. The choice of ΔS^\ddagger as the controlling factor, although reasonable,⁴⁰ is arbitrary. Models equally or more impressive can be constructed with ΔH^\ddagger or a combination of ΔS^\ddagger and ΔH^\ddagger governing the cascade.

Least-Squares Fit to Experimental Data. To examine whether the experimental data themselves are quantitatively consistent with the cascade model for anomalous isotope-effect temperature dependences, we subjected several of the cases studied in this work to a nonlinear least-squares fitting procedure. Because of the limited number and quality of the data, it was necessary to introduce some a priori constraints. Therefore, the fits have to be considered as only illustrative; the particular values of activation parameters and isotope effects which are calculated are not necessarily physically significant.

The procedure used was, first, to assume two kinds of rate-determining steps, one with $\Delta H^\ddagger = 20 \text{ kcal mol}^{-1}$ and one with $\Delta H^\ddagger = 2 \text{ kcal mol}^{-1}$, just as for the HAR and SR steps in the simulation scheme above. Second, it was assumed that only two reaction pathways were important in the temperature intervals studied (about 0 to 65 °C maximum) and that only the low- ΔH^\ddagger step was accessible in this range along one of the pathways. The measured second-order rate constants k_{3H} , for the protiated substrate, were accordingly fitted to eq 7, with ΔS_{A1}^\ddagger , ΔS_{B1}^\ddagger , and ΔS_{A2}^\ddagger obtained as best-fit parameters.⁴¹

$$k_{3H} = (k_{A1}^H k_{B1}^H / [k_{A1}^H + k_{B1}^H]) + k_{A2}^H \quad (7a)$$

$$k_{A1}^H = (kT/h) \exp\{-2000/RT + \Delta S_{A1}^\ddagger/R\} \quad (7b)$$

$$k_{B1}^H = (kT/h) \exp\{-2000/RT + \Delta S_{B1}^\ddagger/R\} \quad (7c)$$

$$k_{A2}^H = (kT/h) \exp\{-2000/RT + \Delta S_{A2}^\ddagger/R\} \quad (7d)$$

Third, it was assumed that the β -D isotope effects were wholly enthalpic, and the measured second-order rate constants k_{3D} , for the deuterated substrate, were fitted to the equations

$$k_{3D} = (k_{A1}^D k_{B1}^D / [k_{A1}^D + k_{B1}^D]) + k_{A2}^D \quad (8a)$$

$$k_{A1}^D = (kT/h) \exp\{-\Delta H_{A1}^\ddagger(3D)/RT + \Delta S_{A1}^\ddagger/R\} \quad (8b)$$

$$k_{B1}^D = (kT/h) \exp\{-\Delta H_{B1}^\ddagger(3D)/RT + \Delta S_{B1}^\ddagger/R\} \quad (8c)$$

$$k_{A2}^D = (kT/h) \exp\{-\Delta H_{A2}^\ddagger(3D)/RT + \Delta S_{A2}^\ddagger/R\} \quad (8d)$$

Note that the values of ΔS^\ddagger from the protiated-substrate reaction were simply carried over so that now $\Delta H_{A1}^\ddagger(3D)$, $\Delta H_{B1}^\ddagger(3D)$, and $\Delta H_{A2}^\ddagger(3D)$ were found as best fit parameters. The calculation can be seen to involve least-squares estimation of the three values of ΔS^\ddagger for the protiated substrate (assuming ΔH^\ddagger 's of 2 and 20 kcal mol⁻¹) and of the three values of ΔH^\ddagger for the deuterated substrate (assuming all ΔS^\ddagger

equal to those for the protiated substrate). Thereafter, the least-squares activation parameters were used to generate values of k_{3H} at any temperature and of the isotope effects k_{3H}/k_{3D} at any temperature. These were used to make "theoretical" plots to compare with the experimental data.

The results for the basic hydrolysis of methyl acetate are shown in Figure 2, where the "theoretical" solid line is compared in the upper panel with the experimental data points for k_{3H} . The broken lines are Eyring plots for the individual rate constants k_{A1}^H , k_{B1}^H , and k_{A2}^H . The best fit ΔS^\ddagger and β -D isotope effects are also shown. The best fit findings, as can be seen, are consistent with an SR rate-determining process at high temperature with a normal β -D effect of $k_{3H}/k_{3D} = 1.02$, an HAR step near room temperature with a very inverse β -D effect of 0.46, and a different SR step, with more negative ΔS^\ddagger and a strongly normal β -D effect of 2.8, at low temperatures. As the lower part of the diagram indicates, the description of the isotope-effect temperature dependence by this model is good at high and medium temperatures. The isotope-effect estimates obtained are not reasonable, but could be brought into a more acceptable range by relaxation of the least-squares criterion. The exercise as it stands, however, demonstrates that the experimental phenomenon of the anomalous temperature dependence in basic ester hydrolysis can be reconciled with a cascading shift among serial and parallel transition states with characteristic normal and inverse isotope effects.

Figure 3 shows the result of a least-squares fit to the data for the basic methanolysis of phenyl acetate. While nonlinearity of the Eyring plot of methyl acetate hydrolysis is visually apparent at the high-temperature end (see Figure 2), the data for the methanolysis of phenyl acetate (Figure 3, upper panel) do not betray any such indication of multiple transition states. Furthermore, the isotope effect (Figure 3, lower panel) is temperature independent to within ± 1 –3% (a "regular" result), except for the apparent upward drift at low and high temperatures, previously mentioned. A least-squares fit to the cascade model nevertheless produces values of ΔS^\ddagger much like those in the methyl acetate case, a prediction of k_{3H} (Figure 3, upper panel, solid line) wholly in accord with the data, and a set of isotope effects (1.19 and 1.25 for the apparent SR steps and 0.75 for the apparent HAR step) which are not far from being reasonable values. The temperature-induced swing of isotope effect (lower panel, solid line) is a good deal more vigorous than the data suggest, but the fit here could be improved by relaxation of the constraints on the activation parameters. We conclude that the cascade model is readily capable of describing acyl-transfer data which generate linear Eyring plots and regular isotope-effect temperature dependences, as well as those in which anomalies are detectable.

Implications of the Cascade Model for Mechanistic Interpretation of β -D Effects. According to the model here advanced, more than one activated complex participates in determining the rate of acyl-transfer reactions in water and methanol around room temperature. Probes of transition-state structure, such as isotope effects, will thus give results which correspond to an averaged structure of the contributing transition states, or a "virtual transition-state structure".²³

Variations in the magnitude of the isotope effect, as a function of reactant structure, solvent, temperature, etc., will arise from a superposition of more primitive changes. Reactant structure, for example, can affect the magnitude of the β -D isotope effect in the following ways:

(a) The structure of each of the contributing transition states can be perturbed to a new equilibrium nuclear geometry either along the reaction coordinate (a parallel or "Hammond" perturbation of structure) or along stable coordinates (perpendicular or "anti-Hammond" perturbations), and in general will suffer a net perturbation which is the resultant of a parallel effect and a number of simultaneous perpendicular effects.³⁹

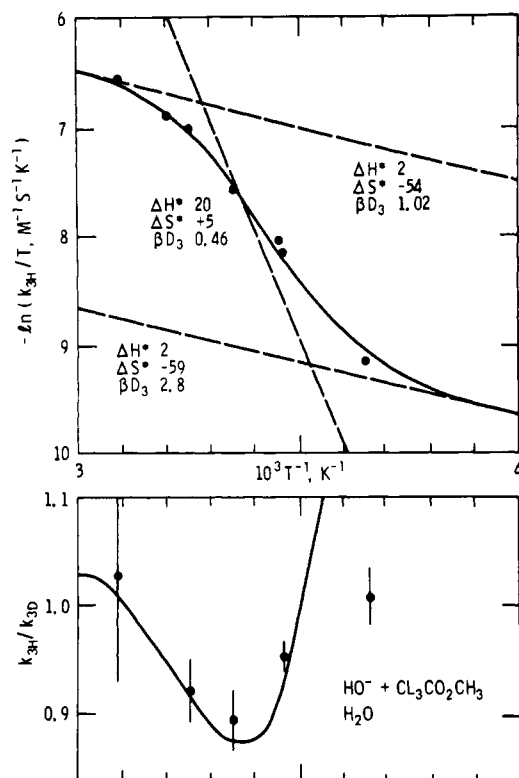


Figure 2. Rate constants for protiated substrate (Eyring plot, upper panel) and β -D secondary isotope effects (lower panel) for basic hydrolysis of methyl acetate ($CH_3CO_2CH_3$, $CD_3CO_2CH_3$) from 0 to 50 °C (data from Table I). The solid lines are calculated from a least-squares fit of the data to a cascade model for the temperature effects.

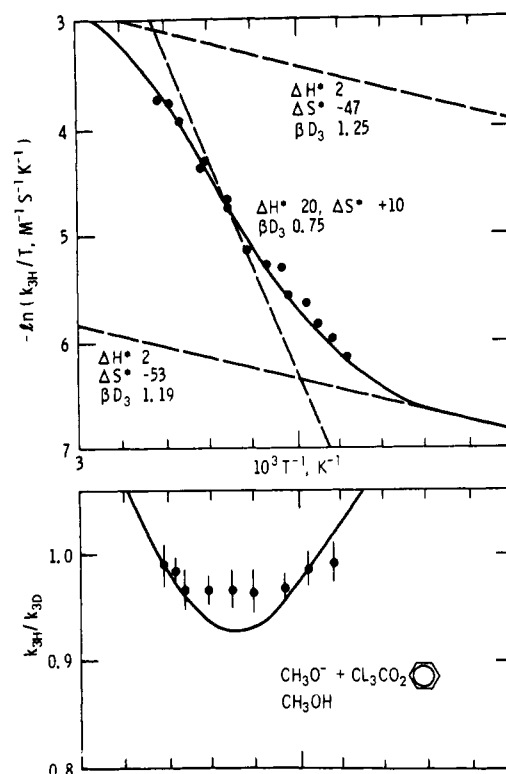


Figure 3. Rate constants for protiated substrate (Eyring plot, upper panel) and β -D secondary isotope effects (lower panel) for basic methanolysis of phenyl acetate (CH_3CO_2Ar , CD_3CO_2Ar) from 5 to 40 °C (data from Table IV). The solid lines are calculated from a least-squares fit of the data to a cascade model for the temperature effects.

For each transition state, this resultant perturbation of its structure will cause its specific or intrinsic β -D isotope effect to be changed.

(b) If the structural alteration of the reactants does not have a sensible effect on the relative free energies of any of the contributing transition states, then their individual weights in determining the rate (and thus in the virtual transition state) will not be changed. In such a case, the observed change in the β -D isotope effect will be a weighted superposition of the changes in the β -D effects for each of the contributing transition states, these changes arising in turn from net structural perturbations that are resultants of parallel and perpendicular perturbations. This may sometimes happen, but, more generally, structural alteration of the reactants will affect the relative free energies of the contributing transition states.

(c) Changes in the relative free energies of serial transition states along a single reaction path will alter the contribution of each to the virtual transition state such that high-free-energy species contribute more heavily.²³ This is analogous to a parallel effect on the structure of a single transition state.

(d) Changes in the relative free energies of transition states in competition, along parallel routes of reaction, will alter the contribution of each to the virtual transition state such that lower free energy species contribute more heavily.²³ This is analogous to a perpendicular effect on the structure of a single transition state. (Note the correlation of parallel effects with serial transition states and perpendicular effects with parallel transition states).

(e) The overall result of a perturbation of the system will therefore be a change in the magnitude of the β -D effect which reflects the altered weights of transition states along serial and parallel routes, with the specific, or intrinsic, isotope effect for each of these transition states itself responding to structural alterations from superimposed perpendicular and parallel effects.

Table VII. β -Deuterium Secondary Isotope Effects for Some Acyl-Transfer Reactions of Acetyl Substrates (CH_3COX , CD_3COX)

reaction, solvent	temp range, °C	k_{3H}/k_{3D}
$HO^- + CL_3CO_2CH_3, H_2O$	~25	0.90 ± 0.02
$H_3O^+ + CL_3CO_2CH_3, H_2O$	0-42	0.93 ± 0.02
$HO^- + CL_3CO_2C_6H_5, H_2O$	5-45	0.98 ± 0.02
$CH_3O^- + CL_3CO_2C_6H_5, CH_3OH$	5-40	0.98 ± 0.02
$CH_3O^- + CL_3CO_2C_6H_4OCH_3(p), CH_3OH$	5-54	0.96 ± 0.02

It should not, therefore, be anticipated that easily interpreted, systematic trends in the magnitude of β -D effects in acyl transfer reactions would result necessarily from changes in reactant structure, solvent, temperature, or other variables. A collection of the kinetic β -D effects determined in this work is presented in Table VII. They can be understood to some degree by assuming (1) that electrophilic interaction, such as solvent removal from near carbonyl carbon in SR steps or protonation in acid-catalyzed reactions, will make a normal ($k_{3H} > k_{3D}$) contribution; (2) that nucleophilic interaction will make an inverse ($k_{3H} < k_{3D}$) contribution, with the value of 0.87 (corrected to three deuteriums) obtained for equilibrium tetrahedral adduct formation representing an approximate limit.⁴²

In this light, we first take note of the fact that all the β -D effects in Table VII are inverse. This corresponds to a predominance of nucleophilic interaction and of HAR (bond formation or bond fission, possibly internal structural relaxation) transition states, at least near 25 °C, for all of these reactions. This is in accord with traditional views of the mechanism.

Both basic and acidic alkyl ester hydrolyses give quite inverse effects, with only a hint of greater electrophilic character for the acid reaction. This corresponds to the traditional idea

of dominance by quasi-tetrahedral, geometrically similar HAR transition states for these two reactions.⁴³ Nucleophilic bonding by water to the protonated carbonyl in the acid-catalyzed reaction has nearly discharged the positive charge on the carbon. This is also in agreement with the small polar effects in acid-catalyzed alkyl ester fission.⁴³

Assuming that a "half-tetrahedral transition state", i.e., one with a bond to the nucleophile which possesses a Pauling bond order of 0.5, would generate the square root of the equilibrium isotope effect for tetrahedral-adduct formation,⁴⁴ one expects $k_{3H}/k_{3D} \sim (0.87)^{1/2} = 0.93$ for such a transition state with no electrophilic contribution. One might then want to conclude that both the basic and acidic alkyl ester hydrolysis transition states are a bit further toward tetrahedral in structure than the halfway point. However, this ought to be taken as a minimal degree of structural progress in the HAR transition state, rather than a quantitative estimate, because any contribution by SR transition states will propel the observed isotope effect in the normal direction.

The basic solvolysis reactions of the three aryl esters show β -D effects not very different from each other but much closer to unity than the effect for the alkyl esters (0.96–0.98 vs. 0.90). If only HAR transition states were important, this would suggest a quasi-trigonal structure with a long, weak bond to the nucleophile. The effect could, however, equally well be produced by a heavier admixture of SR transition states in the aryl ester than in the alkyl ester reactions, and would allow for the structure of the HAR contributor to be little different in the two cases. Such a change in weights in the virtual transition state would in fact be expected. The HAR process should be favored in rate by changing alkyl to aryl; the SR processes ought not to be much affected. The result would be a smaller weight for HAR, and greater weight for SR, transition states with aryl esters. Thus, although the direction of the observed change in β -D effect (indicating a more reactant-like transition state with the approximately tenfold more reactive aryl esters) is that predicted by "Hammond" or parallel effects³⁹ on the structure of a single HAR transition state, it seems more likely to us to have been derived from an increased weight of SR transition states in determining the rate.

Among the aryl esters, there are no definitive variations in β -D effect. The apparent equality of the effects at 0.98 for reaction of phenyl acetate with hydroxide and methoxide ions is consistent with the near equality in rate (methanolysis \sim twofold faster at 25 °C) and the probable similarity in solvation of the two ionic nucleophiles.⁴⁵ SR and HAR transition states of similar structure and weight are likely to compose the virtual transition states. The apparent shift from 0.98 to 0.96 with introduction of the *p*-methoxy group may not be real. It is, however, consistent either with the expected parallel effect in an HAR contributor, or with the expected increased weight of an HAR contributor to the virtual transition state or with a combination of these.

Conclusions

The magnitude and temperature dependences (both regular and anomalous) of the β -deuterium isotope effects for acyl-transfer reactions are understandable in terms of a cascade model, in which a collection of parallel SR–HAR reaction sequences are assumed to compete near room temperature. The apparent properties of the transition state are, on this model, those of a virtual transition state the structure of which is a weighted superposition of contributing SR and HAR transition states. Alterations in the isotope effect (as well as other probes of transition-state structure) then would reflect alterations in the structures of contributing transition states, alterations in the weights of contributing transition states, or most generally both of these.

Experimental Section

Materials and Solutions. Reagent-grade inorganic salts were dried or recrystallized and dried before use. Water was distilled from a copper-bottom still, passed through a Barnstead mixed-bed ion-exchange column, boiled for 20 min, and cooled suddenly. Aqueous sodium hydroxide solutions were diluted from a Fisher certified standard 0.1000 N solution and standardized with potassium hydrogen phthalate. Aqueous perchloric acid solutions were diluted from Mallinckrodt Analytical Reagent perchloric acid (70–72%) and standardized with sodium hydroxide solutions. Titrations were generally conducted in a nitrogen glovebag. Methanol, usually from Fisher or Matheson Coleman and Bell, was purified and sodium methoxide solutions were prepared and used as previously described.⁴⁶ pH measurements employed a Radiometer 26 pH meter.

Substrates. Methyl acetate was prepared by reaction of methanol (Fisher reagent grade, 0.16 mol) with acetic acid (0.18 mol) in the presence of 2 mL of concentrated sulfuric acid, at reflux for 24 h. Collection of the product distilling at 50–57 °C, washing it with 1 mL of saturated aqueous sodium carbonate, drying it over sodium sulfate, and redistillation (52–55 °C) gave about 90% yields. $CD_3CO_2CH_3$, prepared from ICN CD_3CO_2D , produced NMR and mass spectra showing $> 96\%$ deuteration.

1,3-Dichloroacetone (0.2 mol, J. T. Baker, purified by distillation) was stirred with 5 mol of deuterium oxide (Stohler, 99.8% D) containing 0.2 mol of anhydrous sodium acetate (MCB reagent) at room temperature for 20 h in the dark. Extraction with ether, drying with magnesium sulfate, vacuum distillation, and vacuum sublimation gave crystalline material with 90.4% average deuteration (mass spectrum). This substance (0.07 mol) was reexchanged with 1.8 mol of deuterium oxide and 0.07 mol of sodium acetate to produce, after purification, an overall 15% yield of $ClCD_2COCOD_2Cl$ with $94.6 \pm 0.2\%$ deuteration, mp 39.5–40.0 °C.

Phenyl acetate and *p*-methoxyphenyl acetate were prepared from the acid chloride (CH_3COCl from various sources or CD_3COCl , prepared from ICN CD_3CO_2D with thionyl chloride) and the phenol, which had been sublimed. One equivalent of acetyl chloride in dry diethyl ether (distilled from lithium aluminum hydride and stored over sodium) was added to a solution of the phenol in ether containing triethylamine (distilled from potassium hydroxide). The mixture was stirred for several hours at room temperature and washed with 0.1 M hydrochloric acid, 0.1 M sodium bicarbonate, and water. The ether solution was dried with magnesium sulfate and the ether evaporated. The crude esters were dissolved in hot petroleum ether, filtered through neutral alumina, and then chromatographed on neutral alumina with hot petroleum ether eluant to obtain the phenol-free ester, which was then distilled. Mass-spectrometric and NMR analysis indicated a degree of deuteration for the labeled ester of $> 98\%$.

Equilibrium Hydration. 1,3-Dichloroacetone and its deuterated analogue were dissolved in water and in acetonitrile (treated for several days with Linde 4A molecular sieves, twice distilled from phosphorus pentoxide, and stored in the dark in a glovebag under a nitrogen atmosphere) at precisely known concentrations around 0.02 (acetonitrile)–0.08 M (water) in 10 mL volumetric flasks. Dry transfer pipets were used to introduce 3-mL portions into cuvettes. After thermal equilibration in the cell compartment of the Cary 16 spectrophotometer, the ASDAQ system⁴⁷ was used to acquire absorbance data, which were printed in digital form as an average over each 60-s period for 20 min. Acetonitrile samples were observed at 282 nm to obtain the effective extinction coefficient for the ketone $\epsilon = (A_{282}, \text{acetonitrile})/[\text{ketone}, \text{acetonitrile}]$. Values of ϵ around $26 \text{ M}^{-1} \text{ cm}^{-1}$, generally consistent to a few tenths of a percent, were obtained. Aqueous samples were observed at 273 nm. On the assumptions³⁶ of no absorption by the hydrate and that $\epsilon(273, \text{water}) = \epsilon(282, \text{acetonitrile})$, the equilibrium constants K_{4L} ($L = H$ or D) were calculated from

$$K_{4L} = \{[\text{total substrate}, \text{water}]\epsilon / (A_{273}, \text{water})\} - 1$$

Kinetic Measurements. Spectrophotometric measurement of rates with aryl esters was made either with the Cary-16/ASDAQ system⁴⁷ in which a Hewlett-Packard 2100A computer acquires data during the kinetic run or with the Cary-118/SBC 80/10 microcomputer system⁴⁸ in which the BCD output of the Cary 118 is punched on paper tape for later workup in the HP 2100A. First-order rate constants were obtained by a weighted, nonlinear least-squares fit of the data to an exponential function and second-order rate constants from a linear least-squares fit of first-order rate constants to hydroxide or methoxide

concentrations. Temperature control was maintained by circulation of fluid from a Lauda K4/R unit, which bathed the cell compartment, the cell holder, and the syringe from which substrate was injected to initiate the run. The temperatures were digitally monitored, and recorded in analog form, by use of glass-jacketed thermistor probes in the cuvette and syringe jacket.

Titrimetric measurements for alkyl esters were made by removal of aliquots from thermostated reaction vessels, usually 100-mL volumetric flasks, into which substrates had been injected to initiate the reactions. The basic-hydrolysis samples were quenched in excess hydrochloric acid and back-titrated. Typical reaction conditions involved initial methyl acetate concentrations of about 0.013 M and initial sodium hydroxide concentrations of about 0.01 M. Second-order rate constants were found by linear least-squares fitting of the integrated rate law. For the acid-catalyzed reaction, samples were added to a constant amount of standard sodium hydroxide solution and the excess acid was then titrated. Rate constants were obtained by nonlinear least-squares fit to the integrated first-order rate law.

Acknowledgment. We are most grateful to Professor Zafra (Margolin) Lerman for her interest in this work, her kind communication of unpublished data, her critical discussions, and her suggestions.

References and Notes

- (1) This research was supported by grants from the National Institutes of Health and the National Science Foundation and is further described in part: Hogg, J. L. Ph.D. Thesis, University of Kansas, 1974.
- (2) Hogg, J. L. In "Transition States of Biochemical Processes", Gandour, R. D., Schowen, R. L., Eds.; Plenum Press: New York, 1978; Chapter 5.
- (3) Kirsch, J. L. In "Isotope Effects on Enzyme-Catalyzed Reactions", Celand, W. W., O'Leary, M. H., Northrop, D. B., Eds.; University Park Press: Baltimore, 1977; pp 100–121.
- (4) Shiner, V. J., Jr. In "Isotope Effects in Chemical Reactions", Collins, C. J., Bowman, N. S., Eds.; Van Nostrand-Reinhold: Princeton, N.J., 1970; Chapter 2.
- (5) Sunko, D. E.; Borčić, S. In ref 4, Chapter 2.
- (6) Raaen, V. F.; Collins, C. J. *Pure Appl. Chem.* **1964**, *8*, 347–355. Raaen, V. F.; Dunham, T. K.; Thompson, D. D.; Collins, C. J. *Am. Chem. Soc.* **1963**, *85*, 3497–3499. Mislav, K.; Graeve, R.; Gordon, A. J.; Wahl, G. H., Jr. *Ibid.* **1964**, *86*, 1733. Karabatsos, G. J.; Sonnichsen, G. C.; Papioannou, C. G.; Scheppele, S. E.; Shone, R. L. *Ibid.* **1976**, *89*, 463. Carter, R. E.; Melander, L. *Adv. Phys. Org. Chem.* **1973**, *10*, 1–27.
- (7) Halevi, E. A. *Prog. Phys. Org. Chem.* **1963**, *1*, 109–221.
- (8) Kresge, A. J.; Nowlan, V. *Tetrahedron Lett.* **1971**, 4297–4300.
- (9) Arnett, E. M.; Cohen, T.; Bother-By, A. A.; Bushick, R. D.; Sowinski, G. *Chem. Ind. (London)* **1961**, 473–474.
- (10) Maggiora, G. M.; Schowen, R. L. In "Bioorganic Chemistry", van Tamelen, E. E., Ed.; Academic Press: New York, 1977; Vol. 1, Chapter 9.
- (11) Hegazi, M. F.; Quinn, D. M.; Schowen, R. L. In ref 2, Chapter 10.
- (12) Bender, M. L.; Feng, M. S. *J. Am. Chem. Soc.* **1960**, *82*, 6318–6321.
- (13) Jones, J. M.; Bender, M. L. *J. Am. Chem. Soc.* **1960**, *82*, 6322–6326.
- (14) Halevi, E. M.; Margolin, Z. *Proc. Chem. Soc., London* **1964**, 174.
- (15) Wolfsberg, M.; Stern, M. J. *Pure Appl. Chem.* **1964**, *8*, 325–337.
- (16) Stern, M. J.; Spindel, W.; Monse, E. U. *J. Chem. Phys.* **1968**, *48*, 2908–2919.
- (17) Huang, T. T.-S.; Kass, W. J.; Buddenbaum, W. E.; Yankwich, P. E. *J. Phys. Chem.* **1968**, *72*, 4431–4446.
- (18) Spindel, W.; Stern, M. J.; Monse, E. U. *J. Chem. Phys.* **1970**, *52*, 2022–2035.
- (19) Vogel, P. C.; Stern, M. J. *J. Chem. Phys.* **1971**, *54*, 779–796.
- (20) MMI = mass, moment of inertia factor; EXC = excitation factor; ZPE = zero-point energy factor. For an exposition, see Buddenbaum and Shiner.²¹
- (21) Buddenbaum, W. E.; Shiner, V. J., Jr. In ref 3, pp 1–36.
- (22) Thornton, E. R. *Annu. Rev. Phys. Chem.* **1966**, *17*, 349–372. See p 365.
- (23) Schowen, R. L. In ref 2, Chapter 2.
- (24) Winnik, M. A.; Stoute, V.; Fitzgerald, P. J. *Am. Chem. Soc.* **1974**, *96*, 1977. Cf. Stoute, V. A.; Winnik, M. A. *Can. J. Chem.* **1975**, *53*, 3503–3512.
- (25) Congdon, W. I.; Edward, J. T. *Can. J. Chem.* **1972**, *50*, 3921–3923.
- (26) Geneste, P.; Lamaty, G.; Roque, J. P. *Tetrahedron* **1971**, *27*, 5539–5561.
- (27) Küllertz, G.; Fischer, G.; Barth, A. *Tetrahedron* **1976**, *32*, 759–761.
- (28) Fischer, G.; Küllertz, G.; Schellenberger, A. *Tetrahedron* **1976**, *32*, 1503–1505.
- (29) Rossall, B.; Robertson, R. E. *Can. J. Chem.* **1975**, *53*, 869–877. Labels 3 and 4 are interchanged in Figure 1 of this paper.
- (30) Skeptics who consult ref 29 and other reports from Robertson's group will find his one of the few groups legitimately able to claim the precision that supports the maxima and minima here asserted as present.
- (31) Kershner, L. D.; Schowen, R. L. *J. Am. Chem. Soc.* **1971**, *93*, 2014.
- (32) Hopper, C. R.; Schowen, R. L.; Venkatasubban, K. S.; Jayaraman, H. *J. Am. Chem. Soc.* **1973**, *95*, 3280.
- (33) Fairclough, R. A.; Hinshelwood, C. N. *J. Chem. Soc.* **1937**, 538.
- (34) Hornel, J. C.; Butler, J. A. V. *J. Chem. Soc.* **1936**, 1361.
- (35) Nelson, W. E.; Butler, J. A. V. *J. Chem. Soc.* **1938**, 957.
- (36) Greenzaid, P.; Rappoport, Z.; Samuel, D. *Trans. Faraday Soc.* **1967**, *63*, 2131.
- (37) Bell, R. P.; McDougall, A. O. *Trans. Faraday Soc.* **1960**, *56*, 1281.
- (38) A deduction from Hammonds postulate and related ideas.³⁹
- (39) Thornton, E. K.; Thornton, E. R. In ref 2, Chapter 1.
- (40) This particular version of the model is, as stated above, offered only for illustrative purposes and we do not even argue that it is the most physically reasonable choice. However, this combination of ΔS^\ddagger values (most negative for solvent reorganization paired with most positive for heavy-atom reorganization) can be defended physically in several ways. If, for example, the pressure of the most highly constricted solvent shell exerts a "parallel effect"³⁹ on the structure of the bond-formation transition state, it will occur later, with correspondingly greater solvent release.
- (41) Program BMDP3R, UCLA Health Sciences Computing Facility.
- (42) No sensible electrostatic effect from ionization of OH or protonation of O in the tetrahedral adduct is expected: Barnes, D. J.; Goldring, P. D.; Scott, J. M. W. *Can. J. Chem.* **1974**, *52*, 1966.
- (43) Taft, R. W., Jr. In "Steric Effects in Organic Chemistry", Newman, M. S., Ed.; Wiley: New York, 1956; p 588 ff.
- (44) Hogg, J. L.; Rodgers, J.; Kovach, I. M.; Schowen, R. L. *J. Am. Chem. Soc.* **1980**, *102*, 79–85.
- (45) Gold, V.; Grist, S. *J. Chem. Soc., Perkin Trans. 2* **1972**, 89–95.
- (46) Mitton, C. G.; Schowen, R. L.; Gresser, M.; Shapley, J. *J. Am. Chem. Soc.* **1969**, *91*, 2036–2044.
- (47) Hegazi, M. F.; Borchardt, R. T.; Schowen, R. L. *J. Am. Chem. Soc.* **1979**, *101*, 4359–4365.
- (48) Gray, C. H.; Coward, J. K.; Schowen, K. B.; Schowen, R. L. *J. Am. Chem. Soc.* **1979**, *101*, 4351–4358.